

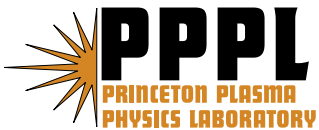
PPPL-4173

PPPL-4173

**A Hypothesis of Inductive Drive to Explain
TEXTOR's Sawtooth Measurements**

T.K. Chu

June 2006



Princeton Plasma Physics Laboratory

Report Disclaimers

Full Legal Disclaimer

This report was prepared as an account of work sponsored by an agency of the United States Government. Neither the United States Government nor any agency thereof, nor any of their employees, nor any of their contractors, subcontractors or their employees, makes any warranty, express or implied, or assumes any legal liability or responsibility for the accuracy, completeness, or any third party's use or the results of such use of any information, apparatus, product, or process disclosed, or represents that its use would not infringe privately owned rights. Reference herein to any specific commercial product, process, or service by trade name, trademark, manufacturer, or otherwise, does not necessarily constitute or imply its endorsement, recommendation, or favoring by the United States Government or any agency thereof or its contractors or subcontractors. The views and opinions of authors expressed herein do not necessarily state or reflect those of the United States Government or any agency thereof.

Trademark Disclaimer

Reference herein to any specific commercial product, process, or service by trade name, trademark, manufacturer, or otherwise, does not necessarily constitute or imply its endorsement, recommendation, or favoring by the United States Government or any agency thereof or its contractors or subcontractors.

PPPL Report Availability

Princeton Plasma Physics Laboratory

This report is posted on the U.S. Department of Energy's Princeton Plasma Physics Laboratory Publications and Reports web site in Fiscal Year 2006.

The home page for PPPL Reports and Publications is:

http://www.pppl.gov/pub_report/

Office of Scientific and Technical Information (OSTI):

Available electronically at: <http://www.osti.gov/bridge>.

Available for a processing fee to U.S. Department of Energy and its contractors, in paper from:

U.S. Department of Energy
Office of Scientific and Technical Information
P.O. Box 62
Oak Ridge, TN 37831-0062

Telephone: (865) 576-8401

Fax: (865) 576-5728

E-mail: reports@adonis.osti.gov

A hypothesis of inductive drive to explain TEXTOR's sawtooth measurements

T. K. Chu^{a)}

Plasma Physics Laboratory, Princeton University, P. O. Box 451,
Princeton, New Jersey 08543

A hypothesis, based on the current density profile determined from the principle of minimum dissipation of magnetic energy, is applied to explain the measurement of $q(0)$ and current variation in a sawtooth cycle in TEXTOR [Plasma Physics and Controlled Nuclear Fusion Research (IAEA, Vienna, 1985), Vol. I, p. 193]. A sawtooth oscillation is triggered when the on-axis current density in a configuration with $m=0$ and $n=0$ symmetry is driven inductively to a limit.

^{a)}Electronic mail: tchu@pppl.gov

I. The TEXTOR measurements

Sawtooth oscillation of electron temperature determined from soft X-ray range of emission in tokamak plasmas was first observed by von Goeler et al. in an ohmic plasma with an on-axis safety factor, $q(r=0) \equiv q_0, < 1$ (r is the minor radius).¹ Its three stages, shown schematically in Fig. 1, are: heating, during which the core temperature of the ($m=0, n=0$) configuration becomes increasingly peaked at the axis; precursor oscillation, during which the amplitude of an off-axis $m=1$ temperature oscillation increases; crash, during which the core temperature profile is flattened (m and n are respectively the poloidal and toroidal mode number). The flattening indicates mixing of magnetic surfaces.

The variation of current density profile,²⁻⁴ Δj_ϕ , in a sawtooth cycle and the global q profile²⁻⁵ were measured by Soltwisch and co-workers in Tokamak Experiment for Technology Oriented Research (TEXTOR)⁶ in a constant-current ohmic plasma. The profiles are obtained from equilibrium calculations that use input signals modelled after the average of the signals measured by a far-infrared polarimeter. The input signals differ from the measured waveforms (see Fig. 5, Ref. 3) near the crash (to $\sim \pm 5\%$ of the sawtooth duration, ~ 20 ms) and near the $q=1$ surface (more so on the weak field side). Thus the profiles (reproduced as Fig. 2 below) do not include the effect of the $m=1$ oscillation prior to the crash or reproduce the immediate-post crash shape. Also not included is

a sheet current at the $q=1$ surface (stronger at the weak-field side) which appears to set in roughly with the precursor, builds up to a peak amplitude at the crash and dies away a few milliseconds after the crash (see p. 480 and Figs. 7 and 5 of Ref. 3).

Figure 2(a) shows Δj_ϕ within the $q=1$ surface in ten equidistant times in a sawtooth cycle and Fig. 2(b), the q profile (the major radius R_0 is 176 cm). The measured results are: $q_0=0.74\pm 0.1$ at the end of the cycle (at t_e); $q_0=0.80\pm 0.1$ at the beginning of the cycle (at t_i); $r_n\approx 11$ cm (the radius of the node of the Δj_ϕ profile), and $r_1\approx 15$ cm (the radius of the $q=1$ surface).

These measurements open up the possibility for a different approach to study sawtooth oscillation. Since the heating stage is identified with current ramping, the onset of the precursor may be triggered by the rising core current instead of pressure. Since the precursor oscillation is identified with a growing poloidal magnetic field perturbation near the $q=1$ surface,⁷ it signifies reconnection of field lines at that surface and hence the growth of an $m=1$ magnetic island.⁸ The crash then may be a result of the island growth.

But the most striking result is the resilience of the q profile. The authors remarked, "the surrounding plasma is hardly affected by the sawtooth activity and acts as a tightly fitting conducting shell."² A comparison of the measured waveforms and the input signals for equilibrium calculations show that within the first couple milliseconds after the crash, while the temperature

profile is still flat, the current configuration has already returned from a presumably different post-crash shape to its pre-precursor shape. This recovery indicates a constraint on the current profile: on a time scale that is longer than about one millisecond (for the TEXTOR parameters), a particular shape of the $(0, 0)$ -symmetry profile prevails. Similar q profiles and q_0 values have been reported by O'Rourke⁹ and Levinton et al.¹⁰

II. The hypothesis

This work proposes that sawtooth oscillation in an ohmic tokamak plasma is inductively driven. The hypothesis permits calculations of q_0 , r_n , r_1 , the induced flux $V_I T_0$ and the shape of the nonuniform toroidal electric field $E_\phi(r)$ that drive the current variation (V_I is inductive voltage and T_0 is the duration of current ramping). The basis for the hypothesis is the time-averaged steady-state current profile of $(0, 0)$ symmetry determined from the principle of minimum dissipation of magnetic energy.¹¹⁻¹³ The variational problem for the principle is formulated for an inductively driven, dissipative toroidal plasma made turbulent by the nested rational magnetic surfaces defined by $q=q_s=m/n$ (m and n are, respectively, the number of poloidal and toroidal turns a field line wraps around the axis before meeting itself). An alternative interpretation of the principle is that the current distribution corresponds to a state of maximum poloidal magnetic field energy (maximum internal inductance) for a

prescribed plasma current. The magnetic field energy of this current profile is defined by q_0 alone (q_0 enters the variational problem in its Lagrange multiplier). If q_0 decreases without limit, the current becomes an on-axis filament current.

But for a q profile to possess the highest internal inductance its on-axis curvature, $q''(0)$, must be positive. Hastie showed that $q''(0)$ changes from positive to negative if q_0 decreases below 0.743.¹⁴ This change is a toroidal effect,¹² shown schematically in Fig. 3. The contribution of terms with $m=0$ symmetry (of terms averaged over the poloidal angle) to $q''(0)$ is positive and independent of q_0 while that of those with $n=0$ symmetry has a $-1/2q_0^2$ dependence; $q''(0)$ becomes negative at a sufficiently low q_0 . This is the q_0 value that marks the end of the $(0, 0)$, and hence the beginning of the $(1, 1)$, symmetry.

To find the q_0 at the beginning of ramping it is necessary to know the amount of magnetic energy that is lost during the precursor stage and the crash. Since the temperature profile is flattened during the crash, we assume that the energy loss is due to a complete magnetic reconnection. Since this loss is a result of configurational change, it does not depend on the speed of reconnection. It can be resistive, as proposed by Kadomtsev,⁸ or collisionless, due to electron inertia¹⁵ or collisionless electron viscosity,¹⁶ or their combination (resistive during the precursor stage and collisionless during the crash).

The model has limitations. The constraint in the variational

problem is constant plasma current, inductively driven. In a plasma with a finite pressure gradient ($\nabla p \neq 0$), diffusion drives a non-inductive current. Thus the constraint requires

$$\nabla p = 0. \tag{1}$$

This condition is well known in plasma studies, but for a different reason. When applied to static equilibrium, $\mathbf{j} \times \mathbf{B} = \nabla p$, it renders the plasma "force-free" (\mathbf{j} is current density and \mathbf{B} is magnetic field). Closed-form solutions for equilibria possessing certain symmetries become obtainable. But no satisfactory answer has been found on why force-free state is the preferred for these plasmas. Here, $\nabla p = 0$ is an idealized approximation to a low-pressure tokamak plasma. Thus the variation is applied to the magnetic energy of a zero pressure, large aspect ratio, circular cross section, and inductive-drive only plasma. The condition is used again in finding the Lagrange multiplier.¹⁴ But for the purpose of finding inductively driven current configuration this condition can be applied to any current-carrying plasma that has negligible diffusion-driven current, such as high-pressure reversed pinch plasmas.¹⁷

III. Calculating q_0 , $V_I T_0$, $E_\phi(r)$

1. The post-crash q_0 . The time-averaged steady-state j_ϕ profile of an inductively driven, dissipative tokamak plasma is^{11,18}

$$\frac{j_{\phi}}{j_{\phi 0}} = \frac{1}{[1 + (q_a/q_0 - 1) r^2/a^2]^2}. \quad (2)$$

The normalized radius of its $q=1$ surface is $r_1/a = [(1 - q_0)/(q_a - q_0)]^{1/2}$ ($r_1 = 14.5$ cm for the TEXTOR parameters). Similarly, the profile within r_1 , for which $q_a = 1$, is,¹³

$$\frac{j_{\phi}}{j_{\phi 0}} = \frac{1}{[1 + (1/q_0 - 1) r^2/r_1^2]^2}. \quad (3)$$

The condition $dj_{\phi}/dq_0 = 0$ gives $r_n/r_1 = [q_0/(1 + q_0)]^{1/2}$ ($r_n = 9.7$ cm for the TEXTOR parameters). Its magnetic energy is

$$W_1 \equiv W(r_1) = \pi a^4 (B_{\phi}/R_0)^2 (\ln q_0^{-1} - 1 + q_0) / 2 (1 - q_0)^2. \quad (4)$$

The pre-reconnection energy ($q_0 = 0.743$) is

$$W_{1,pr} = \pi a^4 (B_{\phi}/R_0)^2 (0.003932). \quad (5)$$

The configurational change due to reconnection has been prescribed by Kadomtsev.⁸ The quantities successively calculated from the current profile are the poloidal magnetic field, the helical magnetic field, the helical magnetic flux, the mixing radius r_m and the magnetic energy within r_m , W_{r_m} . The helical

flux is then inverted (numerically) to obtain the reconnected helical flux. From this flux the post-reconnection magnetic energy $W_{r_m f}$ is obtained. The energy loss is $\Delta W = W_{r_m f} - W_{r_m} - W_{\Delta I}$, where $W_{\Delta I}$ is the magnetic energy associated with the negative current sheet at r_m . For the TEXTOR parameters ($B_\phi = 2.2$ T, $R_0 = 1.76$ m, $a = 0.43$ m, $I_p = 380$ kA, line-averaged electron density $\bar{n}_e = 3.5 \times 10^{13}$ cm⁻³),

$$\Delta W = \pi a^4 (B_\phi / R_0)^2 (-0.00132); \quad (6)$$

it is about one third of $W_{1,pr}$. The available magnetic energy for the post-crash, maximum-inductance configuration is

$$W_{1,po} = \pi a^4 (B_\phi / R_0)^2 (0.002613). \quad (7)$$

The q_0 that corresponds to this energy is $q_{0,po} = 0.791$.

2. The induced flux $V_I T_0$ and the inductive voltage V_I . The sustaining loop voltage within r_1 consists of resistive and inductive component:

$$V_L = I_1 R_\eta + d(L_1 I_1) / dt, \quad (8)$$

where $I_1 = 2\pi r_1^2 B_\phi / \mu_0 R_0$ is the current, R_η is its aggregate resistance, and $L_1 = \mu_0 R_0 (\ln 8 R_0 / a + l_{i1} / 2 - 2)$ is the self-inductance in which l_{i1} is the

internal inductance. For constant I_1 ,

$$V_I = (\mu_0 R_0 / 2) I_1 dl_{i1} / dt. \quad (9)$$

Equation (3) gives $l_{i1} = (q_0 - \ln q_0 - 1) / (1 - q_0)^2$. Its rate of change is $dl_{i1} / dt = f_1(q_0) dq_0 / dt$, where $f_1(q_0) = (q_0 - 2 \ln q_0 - q_0^{-1}) / (1 - q_0)^3$ and $dq_0 / dt \approx -\Delta q_0 / T_0$. The induced magnetic flux during T_0 is

$$V_I T_0 = \pi a^2 [(1 - q_0) / (q_a - q_0)] B_\phi \Delta q_0 f_1(q_0) / 2. \quad (10)$$

For the TEXTOR parameters, with $\Delta q_0 \approx -0.05$,

$$V_I T_0 = 1.86 \times 10^{-3} \text{ V-s}. \quad (11)$$

Use the measured $T_0 \approx 17 \times 10^{-3}$ s and obtain $V_I \approx 0.11$ V. The apparent induced flux is the above value multiplied by the ratio of loop voltage, ~ 1 V, to inductive voltage: $V_L T_0 \approx 1.7 \times 10^{-2}$ V-s.

3. The nonuniform toroidal electric field $E_\phi(r)$. The current variation is usually calculated by solving the current diffusion equation together with an assumption on resistivity.^{9,19,20} Here, since the current profile is known, the shape of the nonuniform field can be obtained by integrating the combined Faraday's and Ampere's equation directly:

$$\frac{1}{r} \frac{\partial}{\partial r} \left(\frac{r \partial E_\phi}{\partial r} \right) = \mu_0 \frac{\partial j_\phi}{\partial t}. \quad (12)$$

Integrate Eq. (12) by using Eq. (3) and obtain

$$E_\phi(r) - E_\phi(0) = -[B_\phi a^2 / 2q_0 R_0 (q_a - q_0)] (dq_0 / dt) F(r), \quad (13)$$

where $F(r) = [(1+b)r^2/r_1^2] / [1+br^2/r_1^2] - \ln(1+br^2/r_1^2) / b^2$, in which $b = 1/q_0 - 1$. It describes the shape of the differential electric field. Figure 4 shows $F(r)$ with $q_0 = 0.77$ (the average value of q_0 during ramping). The node is at $r_n/r_1 \approx 0.66$; j_ϕ increases in time for $r < r_n$ and decreases, for $r > r_n$.

To obtain $E_\phi(r)$, it is necessary to relate it to dissipation at some radius. For $r > r_1$, $V_I = \Delta j_\phi = 0$ (j_ϕ is steady on the time scale of sawtooth period) so that $E_\phi(r) = V_L / 2\pi R_0$. For $r < r_1$, j_ϕ is steady only at the node. Since there cannot be two different E_ϕ values that both correspond to steady-state current density, $E_\phi(r_n) = V_L / 2\pi R_0$. Thus for $r < r_1$,

$$E_\phi(r) = [B_\phi a^2 / 2q_0 R_0 (q_a - q_0)] (dq_0 / dt) [F(r_n) - F(r)] + V_L / 2\pi R_0. \quad (14)$$

The equation can be rearranged to give the ramping period,

$$T_0 = \frac{0.059 B_\phi \pi a^2}{V_L (q_a - q_0) [1 - E_\phi(0) / E_\phi(a)]}, \quad (15)$$

where $[1-E_\phi(0)/E_\phi(a)]$ is a measure of the ratio of the inductive voltage to the loop voltage. A more resistive plasma (due to higher density) leads to longer ramping period.

Figure 5 shows $E_\phi(r)$ of three mid-size tokamaks that have different measured T_0 values: the Princeton Large Torus (PLT),²¹ with $T_0 \sim 5$ ms and $V_L = 1.03$ V ($R_0 = 132$ cm, $a = 40$ cm, $I_p = 490$ kA, $B_\phi = 2.9$ T, and $\bar{n}_e = 1 \times 10^{13}$ cm⁻³);²² the Axially Symmetric Divertor Experiment tokamak (ASDEX),²³ with $T_0 \sim 7$ ms and $V_L = 0.95$ V ($R_0 = 168$ cm, $a = 40$ cm, $I_p = 420$ kA, $B_\phi = 2.8$ T, and $\bar{n}_e = 1.6 \times 10^{13}$ cm⁻³);²⁴ and the TEXTOR. For the PLT parameters the calculated $q_{0,p0}$ is 0.793 and V_I is 0.34 V, and for the ASDEX, they are respectively 0.792 and 0.27 V; $\Delta q_0 \approx -0.05$ in all. The qualitative shape of the profile has been reported by Alladio and Vlad.¹⁹ (In their article the steep drop at $r=r_1$ is replaced by a gradual transition to the region $r > r_1$).

The $E_\phi(0)$ value calculated from Eq. (14) in V/m are ~ 0.051 (PLT), ~ 0.043 (ASDEX) and ~ 0.073 (TEXTOR). Table 1 is a comparison of these values with those calculated from the measured on-axis electron temperature, $T_e(0)$, for two on-axis values of Z_{eff} . There is qualitative agreement if these assumed Z_{eff} are close to reality.

IV. Suggested experiments

1. Constant induced flux. The hypothesis of inductive drive.

cannot give a complete description of sawtooth oscillation because it cannot calculate the dissipative parameter T_0 (or V_L or $T_e(0)$). But $V_I T_0$ being constant can be tested. When lower hybrid wave power is added to an ohmic plasma the loop voltage decreases. Since the current distribution (the inversion radius) does not change when modest amount of wave power is added, constant flux would require T_0 to increase by an amount that maintains the constant.²⁵

2. The consequence of reconnection. The reconnection of field lines at the $q=1$ surface builds an increasingly steep pressure gradient at the boundary that separates the core and the magnetic island.²⁶ In the TEXTOR experiment, is the sheet current at the $q=1$ surface driven by this gradient? Recent measurement of local electron cyclotron emission by Park et al. shows a sharp temperature gradient (not scaled) at the $q=1$ surface near the crash.²⁷ Simultaneous and quantitative measurement of this pressure gradient and the sheet current may lead to a more definitive assertion on whether this pressure gradient, or the onset of some kind of magnetic turbulence,²⁰ causes the crash.

Acknowledgement

I thank Mr. Ron Hatcher for calculating the inverted helical flux function, and Professor Wonhoe Choe for the helpful discussions. The work is supported in part under U.S. Department of Energy Contract No. DE-AC02-76CHO-3073.

Table 1 Comparison of $E_\phi(0)$ based on Eq. (14) and measured $T_e(0)$

Device	measured	$E_\phi(0)$ (V/m)	measured	$E_\phi(0)$ [based on $T_e(0)$] (V/m)	
	T_0 (ms)		$T_e(0)$ (keV) ⁽¹⁾	$Z_{eff}=1$	$Z_{eff}=1.5$
TEXTOR	~17	0.073	~0.9	0.077	0.10
PLT	~5	0.051	~2.0	0.045	0.061
ASDEX	~7	0.043	~1.8 ⁽²⁾	0.039	0.052

(1) $T_e(0)$ varies by ~10%.

(2) Estimated (no Thomson scattering channel at $r=0$).

Appendix: On measured limiting q_0 being different and the disappearance of sawtooth oscillation

The limiting q_0 of a (0, 0) configuration used here, 0.743, is derived for an ohmic plasma having circular cross section, large aspect ratio (defined by the tokamak ordering), zero poloidal beta, and constant plasma current (or, rigorously, the surface voltage does not change on the time scale of sawtooth period). Measured q_0 of ohmic plasmas with circular cross section agrees with this value to ~ 0.05 . The agreement is perhaps somewhat fortuitous as all measurements claim to have an error of ~ 0.1 (their statistical error is ~ 0.05). Measured q_0 in plasmas of non-circular cross section and sustained primarily by energetic neutral-beam particles or radio-frequency waves varies more widely. For example, sawtooth oscillations have been observed in neutral-beam (2.1 MW) heated D-shaped plasma at $q_0 \sim 0.9$.²⁸ Since that diagnostic system had not been used to measure q_0 of a circular ohmic plasma, the effect of non-ohmic drive and non-circular cross section cannot be ascertained. But we can examine the assumptions made in the present analysis and the environment of the experiment to obtain some understanding of the plasma condition that determines its q_0 .

Ellipticity of a cross section has negligible effect on the limiting q_0 and triangulation tends to lower it.¹⁴ But the present hypothesis should not be readily applied to the experiment of Ref. 28 which has substantial non-inductive beam current and diffusion current.

The unsteady experimental condition of Ref. 28 presents another difficulty in knowing the plasma conditions that determine its q_0 . Refer to its Fig. 2. Between shot time 0.6 and 1.0 s, I_p (top trace) is increasing and q_0 (bottom trace) is decreasing, and in the flat-top period between 1.0 to 1.2 s, I_p in fact decreases at a rate ~ -55 kA/s (dq_a/dt is positive) and the change of q_0 in a sawtooth cycle cannot be easily discerned.

In an ohmic-based plasma injected with energetic neutral-beam particles, after the initial rapid drop of surface voltage when the injection begins, its q profile and toroidal electric field profile change continuously for the duration of the injection. Equation (12) relates the boundary condition of these two parameters:²⁹

$$\partial E_\phi / \partial r |_{r=a} = -(\mu_0 I_p / 2\pi a q_a) dq_a / dt, \quad (\text{A1})$$

and

$$\nabla_r^2 E_\phi |_{r=0} = -(2B_\phi / R_0 q_0^2) dq_0 / dt. \quad (\text{A2})$$

The cause of the profile change is the continuous production of the relatively cold electrons born in the core from the injected beam particles. These cold electrons, if they are not transported away from the core, raises the resistivity; the local resistive electric field rises in time. This rise tends to render $E_\phi(r)$ to decrease with radius. If the decreasing trend extends to the

edge, $\partial E_\phi / \partial r|_{r=a}$ is negative and dq_a/dt is positive. Also, $E_\phi(a)$, lagging behind $E_\phi(0)$, must rise in time; the surface voltage increases in time (if the surface voltage is operationally forced to remain constant, the plasma disrupts²⁹). This rise of surface voltage (not shown in Ref. 28) is shown in Fig. 1 of Ref. 30, another experiment with intense beam heating. [The differential between $E_\phi(0)$ and $E_\phi(a)$ results in a particle pinch velocity and hence, "density peaking" (see Fig. 2, Ref. 31).²⁹ Any fueling method that introduces cold electrons to the core, such as pellet injection or cold electrons driven inward by energized antenna when launching radio frequency waves at the plasma periphery, results in such density peaking. To the best of my knowledge, density peaking has not been observed in constant-loop voltage experiments.]

The rise of $E_\phi(r)$ at the axis due to cold electrons also tends to reduce its local concave curvature (refer to Fig. 5). When $\nabla_r^2 E_\phi|_{r=0}$ becomes negative, the (1, 1) configuration sets in, presumably at a q_0 higher than 0.743. Experiments show that as density becomes more peaked at the axis, the limiting q_0 increases continuously from ~ 0.74 .²⁹ Sawtooth oscillation finally disappears at $q_0 \sim 0.8$ as the inversion radius shrinks to zero.

The above description elicits the difficulty in knowing the plasma condition that determines its q_0 in a sawtooth plasma in which the surface voltage is not steady. If the measured $q_0 \sim 0.9$ of Ref. 28 is accurate for a steady-state, beam-heated plasma, we may look for an answer in a minimization analysis that includes

non-inductive current.

A sufficient condition for the elimination of sawtooth oscillation is that $F(r/r_1)$, Fig. 4, is flat. One method is, as described above, adding cold electrons to the core so that the term $[1-E_\phi(0)/E_\phi(a)]$ in Eq. (15) becomes diminishingly small. In a completely non-inductive-drive plasma, there is no sawtooth oscillation because the surface voltage is zero.

References and notes

- ¹ S. von Goeler, W. Stodiek and N. Sauthoff, *Phys. Rev. Lett.* **33**, 1201 (1974).
- ² H. Soltwisch, G. Fuchs, H. R. Koslowski, J. Schlüter, and G. Waidmann, *Proc. 18th Eur. Conf. on Control. Fusion and Plasma Physics*, Berlin 1991, *Europhys. Confs. Vol. 15C*, part II (Eur. Phys. Soc., Geneva, 1991).
- ³ H. Soltwisch, in Contributions to High-Temperature Plasma Physics (Akademie Verlag, Berlin, 1994; ed. K. H. Spatschek and J. Uhlenbusch), p. 471-483.
- ⁴ H. Soltwisch and H. R. Koslowski, *Plasma Phys. Control. Fusion* **37**, 667 (1995); **39** A341 (1997).
- ⁵ H. Soltwisch, W. Stodiek, J. Manickam, and A. Schlüter, Plasma Physics and Controlled Nuclear Fusion Research, 1986, Kyoto (International Atomic Energy Agency, Vienna, 1987), Vol. 1, p. 263.
- ⁶ G. Waidmann, H. L. Bay, G. Bertschinger, W. Bieger, P. Bogen, G. A. Campbell, R. W. Conn, K. H. Dippel, H. G. Esser, K. H. Finken, G. Fuchs, B. Giesen, D. M. Goebel, E. Graffmann, S. E. Guthrie, H. Hartwig, E. Hintz, G. Hrehuss, F. Hoenen, K. Hoethker, A. Kaleck, L. Könen, M. Korten, Y. T. Lie, M. Lochter, M. E. Malinowski, A. E. Pontau, A. Pospieszczyk, U. Samm, B. Schweer, J. Schlüter, H. Soltwisch, H. Van Andel, M. von Hellermann, F. Waelbroeck, L. Wei, J. Winter, G. Wolf, Plasma Physics and Controlled Nuclear Fusion Research, (International Atomic Energy Agency, Vienna, 1985), Vol. I, p. 193.].
- ⁷ H R Koslowski, H Soltwisch and W Stodiek, *Plasma Phys. Control.*

- Fusion **38**, 271 (1996).
- ⁸ B. B. Kadomtsev, *Fiz. Plazmy* **1**, 710 (1975); *Sov. J. Plasma Phys.* **1**, 389 (1975).
- ⁹ J. O'Rourke, *Plasma Phys. Control. Fusion*, **33**, 289 (1991).
- ¹⁰ F. M. Levinton, S. H. Batha, M. Yamada, and M. C. Zarnstorff, *Phys. Fluids B* **5**, 2554 (1993).
- ¹¹ T. K. Chu, *Phys. Plasma* **7**, 3537 (2000); *Phys. Rev. Lett.* **81**, 3148, 5255 (1998).
- ¹² T. K. Chu, *Phys. Plasma* **8**, 3099 (2001).
- ¹³ T. K. Chu, *Phys. Plasma* **9**, 4383 (2002).
- ¹⁴ J. Hastie, *Nucl. Fusion* **29**, 96 (1989).
- ¹⁵ J. Wesson, Plasma Physics and Controlled Nuclear Fusion Research, 1990, Washington (International Atomic Energy Agency, Vienna, 1991), Vol. 2, p. 263.
- ¹⁶ Q. Yu, *Nuclear Fusion* **35**, 1012 (1995).
- ¹⁷ The magnetic configuration of a reversed pinch plasma corresponds to a state of minimum rate of dissipation of magnetic energy for a prescribed rate of dissipation of magnetic helicity (Ref. 11).
- ¹⁸ Equation (2) was first derived by D. Biskamp in *Comments Plasma Phys. Control. Fusion* **10**, 165 (1986), by J. Hsu and M. S. Chu in *Phys. Fluids* **30**, 1221 (1987) and by B. B. Kadomtsev in *Comments Plasma Phys. Control. Fusion* **11**, 153 (1987). [They are a follow-up of the idea of "Profile Consistency" first proposed by B. Coppi in *Comments Plasma Phys. Control. Fusion* **5**, 261 (1980)]. In these three papers, the configuration is thought to be at minimum energy.

- ¹⁹ F. Alladio and G. Vlad, *Phys. Fluids* **31**, 602 (1988).
- ²⁰ F. Porcelli, D. Boucher and M. N. Rosenbluth, *Plasma Phys. Control. Fusion* **38** (1996), 2163.
- ²¹ D. Grove, V. Arunasalam, K. Bol, D. Boyd, N. Bretz, M. Brusati, S. Cohen, D. Dimock, F. Dylla, D. Eames, H. Eubank, B. Fraenkel, J. Girard, R. Hawryluk, E. Hinnov, R. Horton, J. Hosea, H. Hsuan, D. Ignat, F. Jobs, D. Johnson, E. Mazzucato, E. Meservey, N. Sauthoff, J. Schivell, G. Schmidt, R. Smith, F. Stauffer, W. Stodiek, J. Strachan, S. Suckewer, S. von Goeler, K. Young, Plasma Physics and Controlled Nuclear Fusion Research, (International Atomic Energy Agency, Vienna, 1977), Vol. I, p. 21.].
- ²² T. K. Chu, R. Bell, S. Bernabei, A. Cavello, S. Guharay, W. Hooke, J. Hosea, F. Jobs, E. Mazzucato, D. McNeill, E. Meservey, R. Motley, J. Stevens, S. von Goeler, *Nuclear Fusion* **26**, 666 (1986).
- ²³ M. Keilhacker, D. B. Albert, K. Behringer, R. Behrisch, W. Engelhardt, G. Fussmann, J. Gernhardt, E. Glock, G. Hass, G. Herppich, Y. Shie, F. Karger, O. Klüber, M. Kornherr, K. Lackner, G. Lisitano, Ch. Liu, H. M. Mayer, D. Meisel, R. Müller, H. Murmann, H. Niedermeyer, W. Poschenrieder, H. Rapp, S. Rossnagel, J. Roth, N. Ruhs, B. Scherzer, F. Schneider, S. Sesnic, G. Siller, P. Staib, G. Staudenmaier, F. Wagner, K. Wang, H. Wedler, F. Wesner, Plasma Physics and Controlled Nuclear Fusion Research, (International Atomic Energy Agency, Vienna, 1981), Vol. II, p. 351.].
- ²⁴ T. K. Chu and the PBX-M group, *Bull. Am. Phys. Soc.* **37**, 1500 (1992).

- ²⁵ Both the JT-60U tokamak at Japan Atomic Research Institute at Naka, Ibraki, Japan and the HT-7 tokamak at Institute of Plasma Physics at Hefei, China, have the lower hybrid wave system to do the experiment. A localized current drive, such as by waves at electron cyclotron frequency, may be less suitable for the present purpose because it may change the distribution of the current.
- ²⁶ T. K. Chu, Nuclear Fusion, **28**, 1109 (1988)
- ²⁷ H.K. Park, E. Mazzucato, N.C. Luhmann, Jr., C.W. Domier, Z. Xia, T. Munsat, A.J.H. Donné, I.G.J. Classen, and M.J. van de Pol, and the TEXTOR team (to be published in Phys. of Plasmas).
- ²⁸ D. Wróblewski and L. L. Lao, Phys. Fluids B **3**, 2877 (1991).
- ²⁹ T. K. Chu, Phys. Plasmas **4**, 3306 (1997).
- ³⁰ M. C. Zarnstorff, M. G. Bell, M. Bitter, R. J. Goldston, B. Grek, R. J. Hawryluk, K. Hill, D. Johnson, D. McCune, H. Park, A. Ramsey, G. Taylor, and R. Wieland, Phys. Rev. Lett. **60**, 1306, 1988. (In the second half of the duration of the beam injection, dq_a/dt is nearly zero while the surface voltage rises. It means that negative $\partial E_\phi/\partial r$ does not extend to the edge region.)
- ³¹ J. D. Strachan, M. Bitter, A. T. Ramsey, M. C. Zarnstorff, V. Arunasalam, M. G. Bell, N. L. Bretz, R. Budny, C. E. Bush, S. L. Davis, H. F. Dylla, P. C. Efthimion, R. J. Ronck, E. Fredrickson, H. P. Furth, R. J. Goldston, L. R. Grisham, B. Grek, R. J. Hawryluk, W. W. Heidbrink, H. W. Hendel, K. W. Hill, H. Hsuan, K. P. Jaehnig, D. L. Jassby, F. Jobses, D. W. Johnson, L. C. Johnson, R. Kaita, J. Kamperschroer, R. J. Knize, T.

Kozub, H. Kugel, B. LeBlanc, F. Levinton, P. H. La Marche, D. M. Manos, D. K. Mansfield, K. McGuire, D. H. McNeill, D. M. Meade, S. S. Medley, W. Morris, D. Mueller, E. B. Nieschmidt, D. K. Owens, H. Park, J. Schivell, G. Schilling, G. L. Schmidt, S. D. Scott, S. Sesnic, J. C. Sinnis, F. J. Stauffer, B. C. Stratton, G. D. Tait, G. Taylor, H. H. Towner, M. Ultrickson, S. von Goeler, R. Wieland, M. D. Williams, K-L Wong, S. Yoshikawa, K. M. Young, and S. J. Zweben, Phys. Rev. Lett. **58**, 1004 (1987).

Figure captions

Fig. 1. A schematic showing the three stages of a sawtooth oscillation in an ohmic plasma: the current ramping (temperature rising) stage T_0 , the precursor stage of $m=1$ and $n=1$ oscillation T_1 and the crash T_{cr} . In the TEXTOR experiment, $T_0 \sim 17$ ms, $T_1 \sim 2$ ms, and $T_{cr} \sim 100$ μ s.

Fig. 2. The TEXTOR measurements: (a) Δj_ϕ within the $q=1$ surface during a sawtooth cycle in ten equidistant times; (b) q profile. t_i marks the beginning of a sawtooth cycle and t_e , the end.

Fig. 3. A schematic showing the trajectory (the solid line) of the normalized on-axis curvature, $q''(0)/q(0)$, during current ramping stage T_0 as q_0 decreases. The lower half (shaded region) is disallowed as a negative $q''(0)$ would result in a decrease of magnetic energy. The trajectory is the sum of the contributions of terms with $m=0$ symmetry (of terms averaged over the poloidal angle, the upper dashed line) which has no q_0 dependence, and terms with $n=0$ symmetry (the lower dotted line) which varies as $-1/2q_0^2$.

Fig. 4. $F(r/r_1)$, the shape of the toroidal electric field during ramping. r_n is the node at which $F''(r_n/r_1)=0$.

Fig. 5. The calculated toroidal electric field profile: curve (a), TEXTOR; (b), PLT; and (c), ASDEX. (Their respective measured T_0 are 17, 5 and 7 ms.)

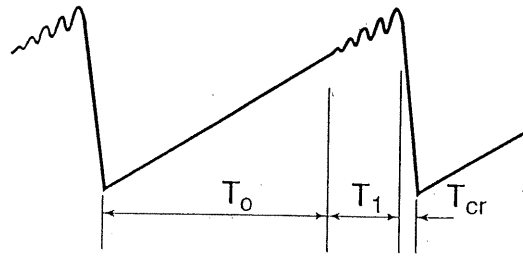


Fig.1

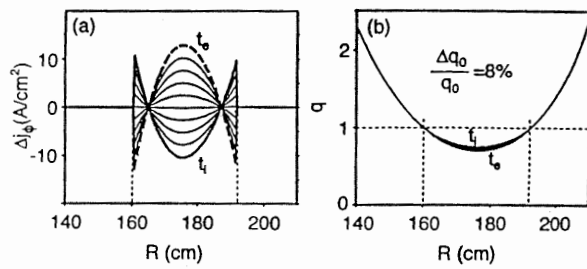


Fig. 2

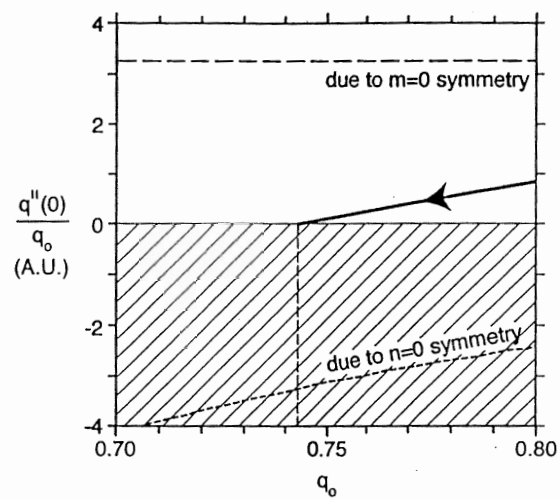


Fig. 3

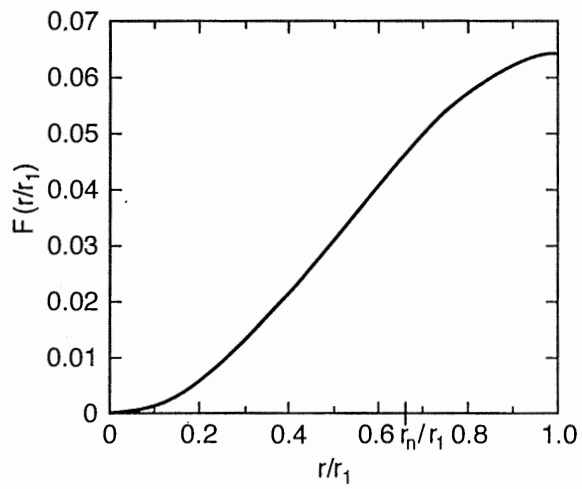


Fig. 4

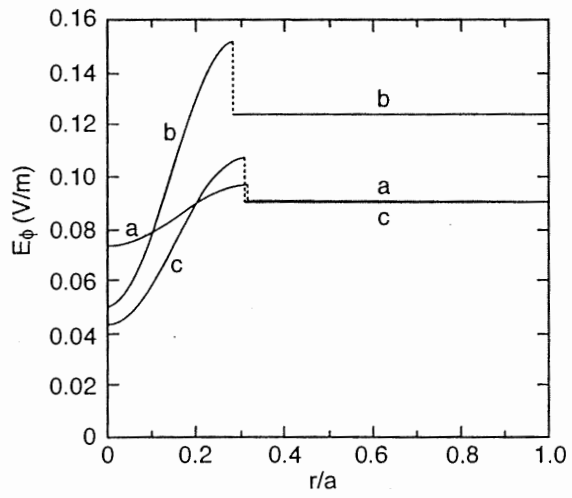


Fig. 5

External Distribution

Plasma Research Laboratory, Australian National University, Australia
Professor I.R. Jones, Flinders University, Australia
Professor João Canalle, Instituto de Fisica DEQ/IF - UERJ, Brazil
Mr. Gerson O. Ludwig, Instituto Nacional de Pesquisas, Brazil
Dr. P.H. Sakanaka, Instituto Fisica, Brazil
The Librarian, Culham Science Center, England
Mrs. S.A. Hutchinson, JET Library, England
Professor M.N. Bussac, Ecole Polytechnique, France
Librarian, Max-Planck-Institut für Plasmaphysik, Germany
Jolan Moldvai, Reports Library, Hungarian Academy of Sciences, Central Research
Institute for Physics, Hungary
Dr. P. Kaw, Institute for Plasma Research, India
Ms. P.J. Pathak, Librarian, Institute for Plasma Research, India
Dr. Pandji Triadyaksa, Fakultas MIPA Universitas Diponegoro, Indonesia
Professor Sami Cuperman, Plasma Physics Group, Tel Aviv University, Israel
Ms. Clelia De Palo, Associazione EURATOM-ENEA, Italy
Dr. G. Grosso, Instituto di Fisica del Plasma, Italy
Librarian, Naka Fusion Research Establishment, JAERI, Japan
Library, Laboratory for Complex Energy Processes, Institute for Advanced Study,
Kyoto University, Japan
Research Information Center, National Institute for Fusion Science, Japan
Professor Toshitaka Idehara, Director, Research Center for Development of Far-Infrared Region,
Fukui University, Japan
Dr. O. Mitarai, Kyushu Tokai University, Japan
Mr. Adefila Olumide, Ilorin, Kwara State, Nigeria
Dr. Jiangang Li, Institute of Plasma Physics, Chinese Academy of Sciences, People's Republic of China
Professor Yuping Huo, School of Physical Science and Technology, People's Republic of China
Library, Academia Sinica, Institute of Plasma Physics, People's Republic of China
Librarian, Institute of Physics, Chinese Academy of Sciences, People's Republic of China
Dr. S. Mirnov, TRINITI, Troitsk, Russian Federation, Russia
Dr. V.S. Strelkov, Kurchatov Institute, Russian Federation, Russia
Kazi Firoz, UPJS, Kosice, Slovakia
Professor Peter Lukac, Katedra Fyziky Plazmy MFF UK, Mlynska dolina F-2, Komenskeho Univerzita,
SK-842 15 Bratislava, Slovakia
Dr. G.S. Lee, Korea Basic Science Institute, South Korea
Dr. Rasulkhozha S. Sharafiddinov, Theoretical Physics Division, Institute of Nuclear Physics, Uzbekistan
Institute for Plasma Research, University of Maryland, USA
Librarian, Fusion Energy Division, Oak Ridge National Laboratory, USA
Librarian, Institute of Fusion Studies, University of Texas, USA
Librarian, Magnetic Fusion Program, Lawrence Livermore National Laboratory, USA
Library, General Atomics, USA
Plasma Physics Group, Fusion Energy Research Program, University of California at San Diego, USA
Plasma Physics Library, Columbia University, USA
Alkesh Punjabi, Center for Fusion Research and Training, Hampton University, USA
Dr. W.M. Stacey, Fusion Research Center, Georgia Institute of Technology, USA
Director, Research Division, OFES, Washington, D.C. 20585-1290

The Princeton Plasma Physics Laboratory is operated
by Princeton University under contract
with the U.S. Department of Energy.

Information Services
Princeton Plasma Physics Laboratory
P.O. Box 451
Princeton, NJ 08543

Phone: 609-243-2750
Fax: 609-243-2751
e-mail: pppl_info@pppl.gov
Internet Address: <http://www.pppl.gov>